The Astrophysical Journal Letters, 774:L6 (5pp), 2013 September 1 doi:10.1088/2041-8205/774/1/L6

ELECTRON-CAPTURE SUPERNOVAE AS SOURCES OF ^{60}Fe

Shinya Wanajo[1], Hans-Thomas Janka[2], and Bernhard Müller[2]
[1] National Astronomical Observatory of Japan, 2-21-1 Osawa, Mitaka, Tokyo 181-8588, Japan; shinya.wanajo@nao.ac.jp
[2] Max-Planck-Institut für Astrophysik, Karl-Schwarzschild-Str. 1, D-85748 Garching, Germany
Received 2013 July 11; accepted 2013 July 29; published 2013 August 13

ABSTRACT

We investigate the nucleosynthesis of the radionuclide ^{60}Fe in electron-capture supernovae (ECSNe). The nucleosynthetic results are based on a self-consistent, two-dimensional simulation of an ECSN as well as models in which the densities are systematically increased by some factors (low-entropy models). ^{60}Fe is found to be appreciably made in neutron-rich ejecta during the nuclear quasi-equilibrium phase with greater amounts being produced in the lower-entropy models. Our results, combining them with the yields of core-collapse supernovae in the literature, suggest that ECSNe account for at least 4%–30% of live ^{60}Fe in the Milky Way. ECSNe co-produce neutron-rich isotopes, ^{48}Ca, ^{50}Ti, ^{54}Cr, some light trans-iron elements, and possibly weak *r*-process elements including some radionuclides such as ^{93}Zr, ^{99}Tc, and ^{107}Pd, whose association with ^{60}Fe might have been imprinted in primitive meteorites or in the deep ocean crust on the Earth.

Key words: nuclear reactions, nucleosynthesis, abundances – stars: abundances – supernovae: general

Online-only material: color figures

1. INTRODUCTION

The origin of the radionuclide ^{60}Fe (halflife of 2.62 Myr; Rugel et al. 2009) has been extensively discussed in connection to gamma-ray astronomy (an overview of the subject can be obtained from Diehl et al. 2011). The 1173 keV and 1332 keV emission from ^{60}Fe decay has been confirmed by the space-based telescopes *RHESSI* (Smith et al. 2004) and *INTEGRAL*/SPI (Harris et al. 2005), indicating ongoing nucleosynthesis of ^{60}Fe in the Milky Way (for recent reviews, see Prantzos 2010; Diehl 2013). The sources of ^{60}Fe have generally been associated with massive stars and subsequent core-collapse supernovae (CCSNe), in which successive neutron captures on Fe isotopes create ^{60}Fe (Timmes et al. 1995; Huss et al. 2009). However, recent CCSN nucleosynthesis calculations (Rauscher et al. 2002; Limongi & Chieffi 2006; Woosley & Heger 2007) predict the ratio of ^{60}Fe to ^{26}Al (halflife of 0.717 Myr) being several times greater than the line flux ratio inferred from the *INTEGRAL*/SPI experiment, $^{60}\mathrm{Fe}/^{26}\mathrm{Al} = 0.148 \pm 0.06$ (Wang et al. 2007). Prantzos (2004) suggested that the discrepancy could be alleviated if the dominant ^{26}Al contributors were Wolf–Rayet star winds that did not eject ^{60}Fe.

A detection of live ^{60}Fe in the deep ocean crust on the Earth has also been recently reported (Knie et al. 2004; Fitoussi et al. 2008), which may be a sign of ^{60}Fe injection from a nearby supernova (SN) into the heliosphere a few Myr ago (Fields et al. 2005, 2008). The origin of live ^{60}Fe in the early solar system has been continuously discussed since its discovery in primitive meteorites (Tachibana & Huss 2003; Mostefaoui et al. 2005; Bizzarro et al. 2007). The initial ratio at the solar birth, $^{60}\mathrm{Fe}/^{56}\mathrm{Fe} \sim 6 \times 10^{-7}$ (e.g., Mishra et al. 2010), appeared to be higher than the interstellar medium (ISM) value, $\sim 3 \times 10^{-7}$ (Huss et al. 2009; Tang & Dauphas 2012).[3] This fact led to an idea that one or several nearby SNe had injected freshly synthesized ^{60}Fe into the early solar system (Wasserburg et al. 1998; Boss & Keiser 2013). A recent meteorite study suggests, however, an initial ratio of $^{60}\mathrm{Fe}/^{56}\mathrm{Fe} \sim 1 \times 10^{-8}$ (see also Moynier et al. 2011; Telus et al. 2012), which is 30 times lower than the ISM value. If this is true, the live ^{60}Fe might have been simply inherited from the ISM to the molecular cloud that made the solar system after a certain decay interval ($\sim$15 Myr; Tang & Dauphas 2012). This assumption, however, needs a mechanism to avoid ^{60}Fe coming from CCSNe during that period of time (see, e.g., Gounelle & Meynet 2012). Vasileiadis et al. (2013) suggested that the low $^{60}\mathrm{Fe}/^{56}\mathrm{Fe}$ ratios were not representative of the proto-solar values.

It should be noted that ^{60}Fe production in CCSN models is subject to uncertainties in several reaction rates (Woosley & Heger 2007; Tur et al. 2010) as well as in the treatment of mass loss, convection, explosion energy, and initial metallicity in stellar models (Limongi & Chieffi 2006; Woosley & Heger 2007). The calculated ^{60}Fe yields should thus be taken with caution. A possible solution to the aforementioned conflicts with observations would thus be that CCSNe actually produced little ^{60}Fe and other sources with longer stellar lifetimes supplied the Galactic ^{60}Fe. Such sources could be asymptotic-giant-branch (AGB, with a C-O core; Wasserburg et al. 2006) or super-AGB (SAGB, with an O-Ne-Mg core; Lugaro et al. 2012) stars, and high-density thermonuclear SNe (SNe Ia; Woosley 1997).

In this Letter, we report that electron-capture SNe (ECSNe; Nomoto 1987; Kitaura et al. 2006; Wanajo et al. 2009), a subclass of CCSNe[4] arising from SAGB stars, can be additional sources of ^{60}Fe in the Milky Way. We adopt our recent nucleosynthesis results of Wanajo et al. (2013) and show that ^{60}Fe is produced in appreciable amounts in the neutron-rich and low-entropy ejecta.

2. ECSN MODEL AND NUCLEOSYNTHESIS

We employ the nucleosynthesis results of Wanajo et al. (2013), which are briefly summarized below. The nucleosynthesis analysis made use of 2000 representative tracer particles, by which the thermodynamic histories of ejecta chunks were followed in our two-dimensional hydrodynamic calculation of an

[3] This value ignores the (highly uncertain) evolution of ^{60}Fe from the solar birth to the present day in the Milky Way (see Huss et al. 2009).

[4] In this Letter, the use of "CCSNe" is restricted to Fe-core-collapse SNe only.

Table 1
Radioactive Yields (in Units of $10^{-5}\ M_\odot$)

Model	^{26}Al	^{41}Ca	^{44}Ti	^{53}Mn	^{60}Fe	^{56}Ni
Unchanged	0.00439	0.0196	0.206	0.111	3.61	293
$f = 1.3$	0.00231	0.0156	0.193	0.108	7.71	340
$f = 2.0$	0.00119	0.00806	0.155	0.0975	13.0	405
CCSNe[a]	4.69	2.10	1.52	26.5	10.4	10800
CCSNe[b]	5.45	...	...	...	8.31	...

Notes.
[a] IMF-averaged CCSN yields, adopting the solar metallicity models of 15–25 $M_\odot$ stars in Rauscher et al. (2002).
[b] IMF-averaged CCSN yields for ^{26}Al and ^{60}Fe, adopting the solar metallicity models of 12–120 $M_\odot$ stars in Brown & Woosley (2013).

ECSN (Janka et al. 2008; Wanajo et al. 2011). Our ECSN model predicts the core-ejecta mass of $1.14 \times 10^{-2}\ M_\odot$ with electron fractions (number of protons per nucleon) of $Y_e \approx 0.40$–0.55 and entropies of $s \approx 13$–$25\ k_B$ nucleon^{-1} (k_B is the Boltzmann constant; see Figure 1 in Wanajo et al. 2013).[5] Post-processing nucleosynthesis calculations with an up-to-date reaction network code (with the reaction library REACLIB version 2.0; Cyburt et al. 2010) predict interesting production of light trans-iron elements (and presumably weak *r*-process elements; Wanajo et al. 2011), whose astrophysical origin has not been fully resolved (see, e.g., Wanajo 2013). A neutron-rich isotope, ^{48}Ca, whose origin remains a long-standing mystery of nucleosynthesis (Meyer et al. 1996; Woosley 1997), is also found to be made in the neutron-rich ejecta with $Y_e \approx 0.40$–0.42 and $s \approx 13$–$15\ k_B$ nucleon^{-1}.

In addition to their "unchanged" ECSN model, Wanajo et al. (2013) also explored models in which the densities were increased by multiplying a constant scaling factor f for all the tracer particles ("$\rho \times f$"). This effectively decreased the entropy by the same factor. It was found that increasing the densities by factors of 1.3 or 2 ($f = 1.3$ or 2, corresponding to a reduction by a factor of 1.3 or 2 in entropy) leads to a remarkable enhancement of the ^{48}Ca abundance. This is a consequence of the fact that a reduction of the entropy turns the nucleosynthesis condition from α-rich QSE (nuclear quasi-equilibrium) to α-poor QSE. In the latter condition, an upward-A shift of the heavy abundances in the QSE cluster is suppressed owing to the paucity of light particles (neutrons, protons, and α's). As a result, ^{48}Ca at the low-A tip of the QSE cluster survives. In this Letter, we also analyze these low-entropy models.

3. ^{60}Fe PRODUCTION IN ECSNe

The final mass fractions of ^{60}Fe are shown in Figure 1 (top) as functions of Y_e along with those for other astrophysically important radionuclides, ^{26}Al, ^{41}Ca, ^{44}Ti, ^{53}Mn, and ^{56}Ni. Among these species only ^{60}Fe forms in the most neutron-rich investigated conditions with $Y_e \approx 0.40$–0.45, which is somewhat isolated from $Y_e \approx 0.46$–0.55 in which the others are produced. These isotopes are made in NSE (nuclear statistical equilibrium) and QSE, and, in part, by α and proton captures after the QSE freezeout. The smaller core-ejecta mass of an ECSN results in several 10 times smaller amounts of these isotopes (first line in Table 1) than in CCSNe (fourth and fifth lines in Table 1, in which the abundances taken from Rauscher et al. 2002; Brown & Woosley 2013, are mass-averaged by the stellar initial mass function, IMF; see Section 4).

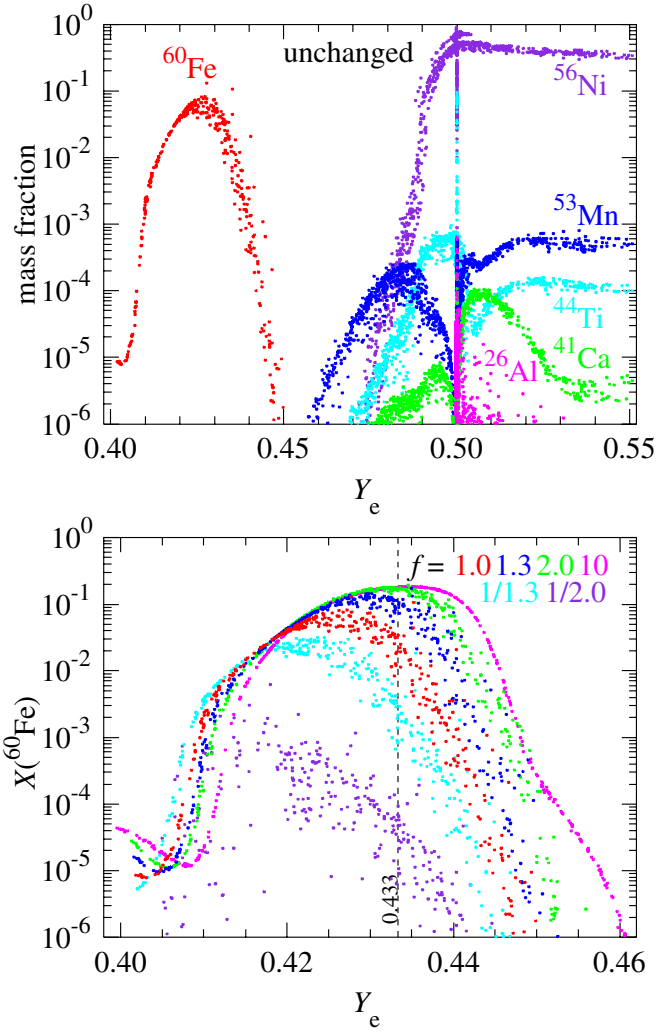

Figure 1. Top: final mass fractions of radionuclides ^{26}Al, ^{41}Ca, ^{44}Ti, ^{53}Mn, ^{60}Fe, and ^{56}Ni for all the tracer particles of the unchanged ECSN model as functions of Y_e. Bottom: final mass fractions of ^{60}Fe for the tracer particles in the range of $Y_e < 0.462$. Also indicated by a dashed line is $Y_{e,nuc} = 0.433$. The result of the unchanged model ($f = 1$) is shown in red, and those with the densities multiplied by scaling factors $f = 1.3$, 2.0, 10, 1/1.3, and 1/2.0 are given in different colors.
(A color version of this figure is available in the online journal.)

Despite the small core-ejecta mass, we find a similar amount of ^{60}Fe for ECSNe comparable to that for CCSNe. This is due to appreciable production of ^{60}Fe in QSE with neutron-rich conditions for $Y_e \sim Y_{e,nuc} = 26/60 = 0.433$ (characterizing the structure of ^{60}Fe), which is absent in CCSN ejecta. In fact, ^{60}Fe is the most tightly bound isotope in the range $Y_{e,nuc} < 0.438$. The mass fraction $X(^{60}\mathrm{Fe})$, however, peaks at $Y_e = 0.428$, which is slightly below 0.433 (red dots in Figure 1, bottom). This is due to the presence of a more tightly bound isotope ^{64}Ni with $Y_{e,nuc} = 0.438$.

Figure 2 elucidates the nuclear evolutions for two representative tracer particles with $Y_e = 0.433$ (a) and 0.428 (b). The entropies are $s = 14.9\ k_B$ nucleon^{-1} and $13.6\ k_B$ nucleon^{-1}, respectively. The expansion timescales, defined as the e-folding times of the temperature drop below 0.5 MeV, are $\tau_{exp} = 63.8$ ms and 61.8 ms, respectively. The abundances (number per nucleon, $Y \equiv X/A$) of α, ^{60}Fe, and heavy nuclei ("h," $A > 4$)

[5] Throughout this Letter, Y_e and s are evaluated when the temperatures drop to 5 GK.

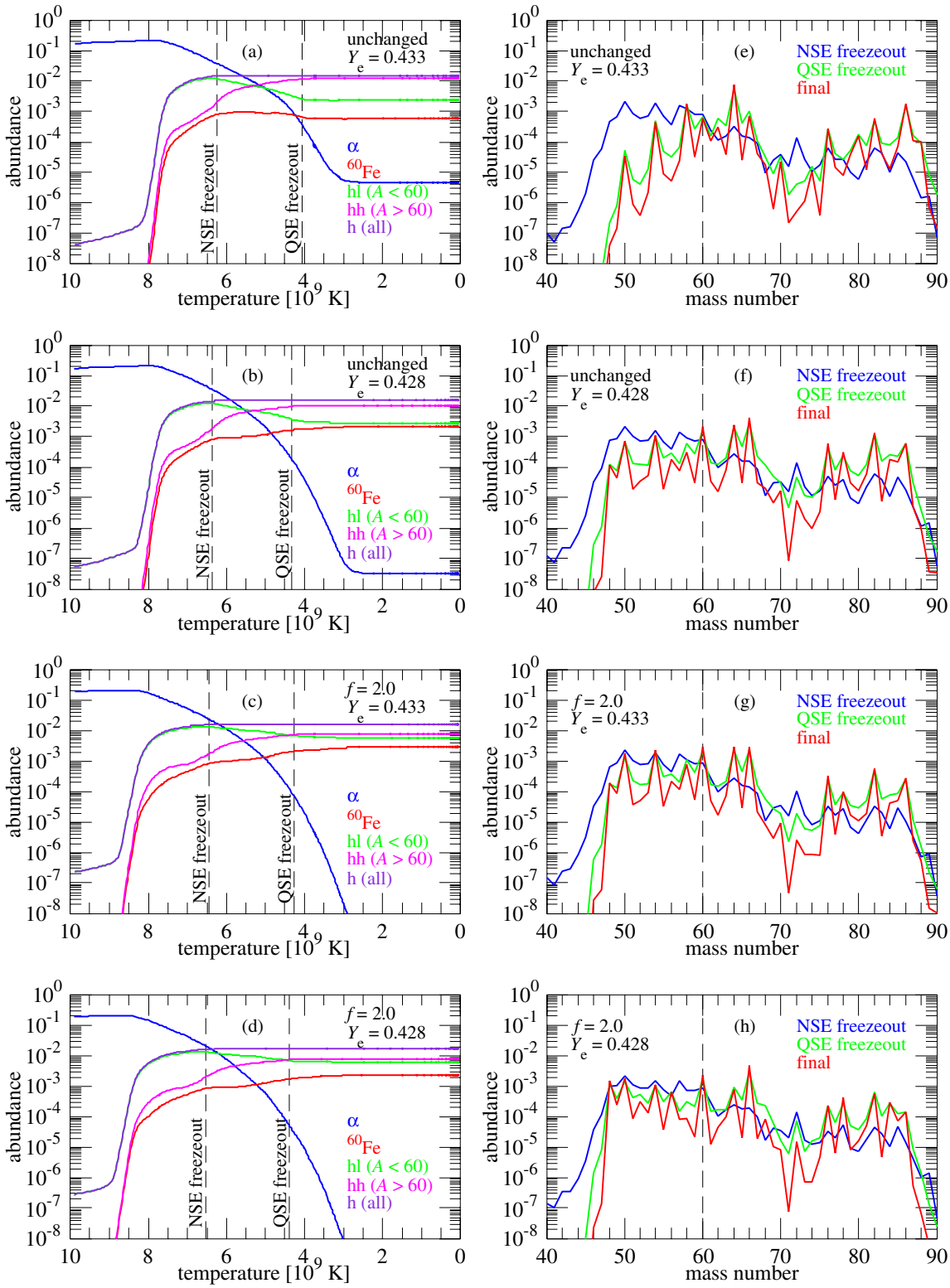

Figure 2. Left: abundances of α, ^{60}Fe, and heavy nuclei (for $A < 60$, $A > 60$, and all the range) as functions of descending temperature for the tracer particles with $Y_e = 0.433$ ((a) and (c)) and 0.428 ((b) and (d)) of the unchanged model ((a) and (b)) and those for $f = 2.0$ ((c) and (d)). The long-dashed lines mark the NSE-freezeout and QSE-freezeout temperatures. Right: nuclear abundances at the NSE freezeout, at the QSE freezeout, and at the end of calculations for the same tracer particles ((e)–(h)). The dashed line in each panel marks the position of ^{60}Fe.

(A color version of this figure is available in the online journal.)

are drawn as functions of descending temperature. Also shown are the abundances of heavy nuclei with $A < 60$ ("hl") and with $A > 60$ ("hh"). We find that the heavy abundance, Y_h, approaches a constant value around 6 GK. This is a freezeout from NSE, defined here when the timescale of heavy abundance formation, $\tau_h \equiv Y_h/\dot{Y}_h$, exceeds τ_{exp}.

We realize an upward-A shift of the heavy abundances after the NSE freezeout from decreasing Y_{hl} and increasing Y_{hh} in

Figures 2(a) and (b). This is a result of the α-rich freezeout from NSE (Woosley & Hoffman 1992) followed by QSE (Meyer et al. 1998), recognized by $Y_\alpha/Y_h = 2.57$ and 2.33 at the NSE freezeout for the $Y_e = 0.433$ and 0.428 cases, respectively. We define the QSE freezeout when the timescale of the abundance formation for $A > 60$, $\tau_{hh} \equiv Y_{hh}/\dot{Y}_{hh}$, exceeds τ_{exp}. QSE freezes out typically around 4 GK (Meyer et al. 1998) and the upward-A shift of the heavy abundances ceases.

We find in Figures 2(a) and (b) that the ^{60}Fe abundances for $Y_e = 0.433$ and $Y_e = 0.428$, respectively, decrease and increase during the QSE phase. Figures 2(e) and (f) clarify the reason, illustrating the nuclear abundances at the NSE freezeout, at the QSE freezeout, and at the end of calculation for each tracer particle. We find that, at the NSE freezeout, ^{60}Fe belongs to the lighter group of the NSE cluster.

For the $Y_e = 0.433$ case (Figures 2(a) and (e)), a drastic upward-A shift of the heavy abundances takes place during the QSE phase. As a result, a part of the ^{60}Fe abundance is taken by the heavier group, in particular by ^{64}Ni. For the $Y_e = 0.428$ case (Figures 2(b) and (f)), the upward-A shift is smaller as a result of the smaller Y_α/Y_h at the NSE freezeout. More importantly, the Y_e is appreciably smaller than the $Y_{e,nuc}$ of ^{64}Ni, making ^{60}Fe the most tightly bound isotope in this condition. As a result, ^{60}Fe keeps increasing in the QSE cluster and even after the QSE freezeout.

In summary, ^{60}Fe forms in NSE and further increases or decreases in QSE depending on the neutron-richness as well as the available number of α's during the QSE phase. The latter condition is closely related to entropy. In the following, we thus inspect the ECSN models in which densities are multiplied by a scaling factor f for all the tracer particles.

Figure 1 (bottom) shows the final mass fractions of ^{60}Fe for the unchanged model ($f = 1$) and those with $f = 1.3$, 2.0, 10, 1/1.3, and 1/2.0. We find a strong sensitivity of the ^{60}Fe production to entropy. The nuclear evolutions for $f = 2.0$ are presented in Figure 2(c) for $Y_e = 0.433$ and in Figure 2(d) for 0.428. The Y_α/Y_h ratios at the NSE freezeout are 1.46 and 1.33, respectively, being only slightly greater than unity, as a result of reduced entropies by about a factor of two. As a result, an upward-A shift of the abundances is restricted by a small number of light particles. ^{60}Fe thus survives and increases during the QSE phase, being maximal around $Y_{e,nuc} = 0.433$ (Figure 1, bottom).

The resulting ejecta masses of radionuclides for $f = 1.3$ and 2.0 are presented in Table 1 (second and third lines). ^{60}Fe is appreciably produced in the low-entropy models. A decrease of only about 30% in entropy doubles the ejecta mass of ^{60}Fe, being comparable to that for CCSNe. About a factor of two decrease in entropy leads to about four times greater ^{60}Fe amount, being already close to that for the extreme, $f = 10$ case ($1.40 \times 10^{-4}\,M_\odot$; not presented in Table 1). The ejecta mass of $M_{ej}(^{60}\mathrm{Fe}) \sim 1 \times 10^{-4}\,M_\odot$ can thus be taken to be the upper limit for ECSNe.

4. CONTRIBUTION TO GALAXY AND SOLAR SYSTEM

The contribution of ECSNe to the Galactic ^{60}Fe depends on the mass window leading to SNe from the stellar SAGB mass range (Nomoto 1987; Siess 2007; Poelarends et al. 2008). From their stellar evolution models, Poelarends et al. (2008) obtained the initial mass range for SAGB stars to be 7.5–9.25 $M_\odot$ in the solar metallicity case. Assuming that all this range leads to the SN channel, the fraction of ECSNe relative to all SN events (ECSNe + CCSNe) becomes $f_{ECSN} = 0.253$ by adopting the Salpeter IMF ($\propto M_{star}^{-2.35}$) with the upper-end of 120 $M_\odot$.[6] This can be regarded as the absolute upper limit of f_{ECSN} in the local universe with the metallicity near the solar value.

Table 2
Most Overproduced Isotopes and ECSN Contributions

Model	Isotope	$X/X_\odot$	f_{ECSN}	f_{60Fe}	^{60}Fe/^{26}Al[a]
Unchanged	^{86}Kr	355	0.0854	0.0391	0.0268
$f = 1.3$	^{74}Se	125	0.165	0.155	0.121
$f = 2.0$	^{48}Ca	80.9	0.240	0.332	0.328

Note. [a] Number ratios by assuming $f_{60Fe} = 1$ (see the text).

We further evaluate the upper limit on f_{ECSN} based on our result. For the unchanged model, the most overproduced isotope relative to the solar value is ^{86}Kr (Table 2, first line). Given that ^{86}Kr in the Milky Way was exclusively made by ECSNe, we have (Wanajo et al. 2011),

$$\frac{f_{ECSN}}{1 - f_{ECSN}} = \frac{X_\odot(^{86}\mathrm{Kr})/X_\odot(^{16}\mathrm{O})}{M_{ECSN}(^{86}\mathrm{Kr})/M_{CCSN}(^{16}\mathrm{O})}, \quad (1)$$

where $X_\odot(^{86}\mathrm{Kr}) = 2.39 \times 10^{-8}$ and $X_\odot(^{16}\mathrm{O}) = 6.60 \times 10^{-3}$ are the mass fractions of these isotopes in the solar system (Lodders 2003). $M_{ECSN}(^{86}\mathrm{Kr}) = 6.23 \times 10^{-5}\,M_\odot$ is the ^{86}Kr mass for the unchanged ECSN model. $M_{CCSN}(^{16}\mathrm{O}) = 1.63\,M_\odot$ is the IMF-averaged ^{16}O mass per CCSN event, in which the yields are taken from Brown & Woosley (2013, their Table 1).[7] With these values, we get $f_{ECSN} = 0.0854$ for the unchanged model. For the low-entropy models with $f = 1.3$ and 2.0, Equation (1) gives $f_{ECSN} = 0.165$ and 0.240, respectively, by replacing ^{86}Kr with the most overproduced isotopes, ^{74}Se and ^{48}Ca.

Taking the IMF-averaged ^{60}Fe mass, $M_{CCSN}(^{60}\mathrm{Fe}) = 8.31 \times 10^{-5}\,M_\odot$ with the CCSN yields in Brown & Woosley (2013), the fractions of the Galactic ^{60}Fe from ECSNe (relative to that from all SN events) become $f_{60Fe} = 0.0391$, 0.155, and 0.332 for the unchanged, $f = 1.3$, and $f = 2.0$ cases, respectively. This indicates that ECSNe supply about 4%–30% of live ^{60}Fe in the Milky Way. It should be noted that the ratio from the CCSN yields, ^{60}Fe/^{26}Al = 0.661, is already more than four times greater than the observational flux ratio of 0.148 (Wang et al. 2007). A contribution from ECSNe would thus enlarge the discrepancy. As noted in Section 1, however, ^{60}Fe production in CCSNe is subject to uncertainties in several reaction rates as well as in astrophysical modeling of stellar evolution. Contributions from ECSNe could therefore be greater than the above estimate. As an extreme case, we provide the ratios of ^{60}Fe/^{26}Al with no ^{60}Fe (but ^{26}Al) contribution from CCSNe (i.e., $f_{60Fe} = 1$) in Table 2 (last column). We find that the low-entropy model with $f = 1.3$ gives the value that is roughly consistent with the gamma-ray observation.

If the Galactic ^{60}Fe were exclusively produced by ECSNe, their longer progenitor lifetimes (>15 Myr) could give rise to different distributions between ^{26}Al and ^{60}Fe. On the one hand, the ^{26}Al distribution appears to be clumpy as evidenced by the *INTEGRAL*/SPI mission (Diehl 2013). Some of this clumpiness is associated with regions hosting many young, massive stars such as the Cygnus region. On the other hand, ^{60}Fe may not be associated with such young stellar regions and

[6] The result is not very sensitive to this value. The upper-mass of 40 $M_\odot$, e.g., gives $f_{ECSN} = 0.275$.
[7] This is a subset of the yields from the "A" series in Woosley & Heger (2007).

thus be distributed more diffusely. Although the Cygnus region marginally appears within the *INTEGRAL* sensitivity for ^{60}Fe, no signal of its decay has been found (Martin et al. 2010). This could be due to the age of the Cygnus complex being much younger than the lifetimes of ECSN progenitors.

The signatures of ^{60}Fe production in ECSNe might have been imprinted also in primitive meteorites or in the deep ocean crust. ECSNe produce appreciable ^{48}Ca (also ^{50}Ti and ^{54}Cr; Wanajo et al. 2013) that cannot be made by CCSNe. Its association with excess ^{60}Fe could thus be a sign of the ECSN origin. In fact, such a correlation in meteorites was reported by Chen et al. (2011). Note, however, that both ^{60}Fe and ^{48}Ca could also originate from a rare class of high density SNe Ia (Woosley 1997). Our ECSN model, however, produces almost all light trans-iron nuclei up to $Z = 40$ (Figure 5 in Wanajo et al. 2013) and presumably weak *r*-process nuclei up to $Z = 50$ (Figure 5 in Wanajo et al. 2011). The latter can also be created in the subsequent neutrino-driven outflows (Wanajo 2013). The weak *r*-process products should include a few radionuclides with lifetimes comparable to that of ^{60}Fe, such as ^{93}Zr (1.53 Myr), ^{99}Tc (0.211 Myr), and ^{107}Pd (6.5 Myr). Therefore, it will be crucial to find correlations also with these trans-iron species that are not made by SNe Ia.

5. SUMMARY

We examined the production of ^{60}Fe in ECSNe in connection to the nucleosynthetic results of Wanajo et al. (2013). The models were based on the two-dimensional core-collapse simulation (Janka et al. 2008; Wanajo et al. 2011) of an 8.8 $M_\odot$ SAGB star (Nomoto 1987). In addition to the unchanged ECSN model, we adopted the low-entropy models of Wanajo et al. (2013), in which densities were multiplied by a factor *f*. We found appreciable ^{60}Fe production during the NSE and subsequent QSE phases in the neutron-rich ejecta with $Y_e \sim 0.43$. The amount of ^{60}Fe is highly dependent on entropy; lower entropy models ($f = 1.3$ and 2.0) make more ^{60}Fe.

The unchanged ECSN model predicted ∼4% contribution of ECSNe (relative to all SN events) to the Galactic ^{60}Fe. This fraction could increase to ∼30% (for $f = 2.0$) if the low-entropy models were adopted. If this were the case, the Galactic flux ratio of ^{60}Fe/^{26}Al = 0.148 (Wang et al. 2007) would be explained without ^{60}Fe contributions from CCSNe. If the Galactic ^{60}Fe were dominantly supplied from ECSNe (i.e., the CCSN yields were severely overestimated), ^{60}Fe would be more diffusely distributed than ^{26}Al without showing clear associations with young stellar regions such as the Cygnus complex. This should be confirmed by future gamma-ray line surveys.

Our ECSN models co-produce the neutron-rich isotope ^{48}Ca (Wanajo et al. 2013), light trans-iron elements, and possibly weak *r*-process elements (Wanajo et al. 2011; Wanajo 2013), accompanied by several radionuclides with million-year lifetimes (e.g., ^{93}Zr, ^{99}Tc, and ^{107}Pd). Correlations between ^{60}Fe and these isotopes in primitive meteorites (Chen et al. 2011) or in the deep ocean crust on the Earth (Knie et al. 2004; Fitoussi et al. 2008) will be an invaluable evidence of ^{60}Fe production in ECSNe.

Finally, it should be cautioned that further improvements of hydrodynamical models (e.g., three-dimensional, high-resolution, and general-relativistic treatment) will be needed before drawing more firm conclusions. Studies of ^{60}Fe production by a mini *s*-process during the SAGB stage (Lugaro et al. 2012) prior to ECSN explosions are also important to evaluate the net ^{60}Fe ejecta from such stars.

S.W. was supported by the JSPS Grants-in-Aid for Scientific Research (23224004). At Garching, support by Deutsche Forschungsgemeinschaft through grants SFB/TR7 and EXC-153 is acknowledged.

REFERENCES

Bizzarro, M., Ulfbeck, D., Trinquier, A., et al. 2007, Sci, 316, 1178
Boss, A. P., & Keiser, S. A. 2013, ApJ, 770, 51
Brown, J. M., & Woosley, S. E. 2013, ApJ, 769, 99
Chen, H.-W., Lee, T., Lee, D.-C., Jiun-San Shen, J., & Chen, J.-C. 2011, ApJL, 743, L23
Cyburt, R. H., Amthor, A. M., Ferguson, R., et al. 2010, ApJS, 189, 240
Diehl, R. 2013, RPPh, 76, 026301
Diehl, R., Hartmann, D., & Prantzos, N. (ed.) 2011, Astronomy with Radioactivities (Lecture Notes in Physics, Vol. 812; Berlin: Springer)
Fields, B. D., Athanassiadou, T., & Johnson, S. R. 2008, ApJ, 678, 549
Fields, B. D., Hochmuth, K. A., & Ellis, J. 2005, ApJ, 621, 902
Fitoussi, C., Raisbeck, G. M., Knie, K., et al. 2008, PhRvL, 101, 121101
Gounelle, M., & Meynet, G. 2012, A&A, 545, A4
Harris, M. J., Knödlseder, J., Jean, P., et al. 2005, A&A, 433, L49
Huss, G. R., Meyer, B. R., Srinivasan, G., Goswami, J. N., & Sahijpal, S. 2009, GeCoA, 73, 4922
Janka, H.-Th., Müller, B., Kitaura, F. S., & Buras, R. 2008, A&A, 485, 199
Kitaura, F. S., Janka, H.-Th., & Hillebrandt, W. 2006, A&A, 450, 345
Knie, K., Korschinek, G., Faestermann, T., et al. 2004, PhRvL, 93, 1103
Limongi, M., & Chieffi, A. 2006, ApJ, 647, 483
Lodders, K. 2003, ApJ, 591, 1220
Lugaro, M., Doherty, C. L., Karakas, A. I., et al. 2012, M&PS, 47, 1998
Martin, P., Knödlseder, J., Meynet, G., & Diehl, R. 2010, A&A, 511, A86
Meyer, B. S., Krishnan, T. D., & Clayton, D. D. 1996, ApJ, 462, 825
Meyer, B. S., Krishnan, T. D., & Clayton, D. D. 1998, ApJ, 498, 808
Mishra, R. K., Goswami, J. N., Tachibana, S., Huss, G. R., & Rudraswami, N. G. 2010, ApJL, 714, L217
Mostefaoui, S., Lugmair, G. W., & Hoppe, P. 2005, ApJ, 625, 271
Moynier, F., Blichert-Toft, J., Wang, K., Herzog, G. F., & Albarede, F. 2011, ApJ, 741, 71
Nomoto, K. 1987, ApJ, 322, 206
Poelarends, A. J. T., Herwig, F., Langer, N., & Heger, A. 2008, ApJ, 675, 614
Prantzos, N. 2004, A&A, 420, 1033
Prantzos, N. 2010, in 8th INTEGRAL Workshop "The Restless Gamma-ray Universe"—Integral2010 (PoS; Trieste: SISSA), 018
Rauscher, T., Heger, A., Hoffman, R. D., & Woosley, S. E. 2002, ApJ, 576, 323
Rugel, G., Faestermann, T., Knie, K., et al. 2009, PhRvL, 103, 072502
Siess, L. 2007, A&A, 476, 893
Smith, D. M. 2004, in 5th INTEGRAL Workshop on the INTEGRAL Universe, ed. V. Schoenfelder, G. Lichti, & C. Winkler (ESA SP-552; Noordwijk: ESA), 45
Tachibana, S., & Huss, G. R. 2003, ApJL, 588, L41
Tang, H., & Dauphas, N. 2012, E&PSL, 359, 248
Telus, M., Huss, G. R., Ogliore, R. C., Nagashima, K., & Tachibana, S. 2012, M&PS, 47, 2013
Timmes, F. X., Woosley, S. E., Hartmann, D. H., et al. 1995, ApJ, 449, 204
Tur, C., Heger, A., & Austin, S. M. 2010, ApJ, 718, 357
Vasileiadis, A., Nordlund, Å., & Bizzarro, M. 2013, ApJL, 769, L8
Wanajo, S. 2013, ApJL, 770, L22
Wanajo, S., Janka, H.-T., & Müller, B. 2011, ApJL, 726, L15
Wanajo, S., Janka, H.-T., & Müller, B. 2013, ApJL, 767, L26
Wanajo, S., Nomoto, K., Janka, H.-T., Kitaura, F. S., & Müller, B. 2009, ApJ, 695, 208
Wang, W., Harris, M. J., Diehl, R., et al. 2007, A&A, 469, 1005
Wasserburg, G. J., Busso, M., Gallino, R., & Nollett, K. M. 2006, NuPhA, 777, 5
Wasserburg, G. J., Gallino, R., & Busso, M. 1998, ApJL, 500, L189
Woosley, S. E. 1997, ApJ, 476, 801
Woosley, S. E., & Heger, A. 2007, PhR, 442, 269
Woosley, S. E., & Hoffman, R. D. 1992, ApJ, 395, 202